Specific interaction to PIP2 increases the kinetic rate of membrane binding of VILIPs, a subfamily of Neuronal Calcium Sensors (NCS) proteins

Author

Rebaud, Samuel, Wang, Conan K, Sarkis, Joe, Mason, Lyndel, Simon, Anne, Blum, Loic J, Hofmann, Andreas, Girard-Egrot, Agnes P

Published

2014

Journal Title

Biochimica et Biophysica Acta: international journal of biochemistry and biophysics

DOI

10.1016/j.bbamem.2014.06.021

Specific interaction of N-terminal polybasic cluster to PIP_2 increases the kinetic rate of membrane binding of VILIPs, a subfamily of Neuronal Calcium Sensors (NCS) proteins

Samuel Rebaud[1], Conan K. Wang[2], Joe Sarkis[1], Lyndel Mason[2], Anne Simon[1], Loïc J. Blum[1], Andreas Hofmann[2,3], Agnès P. Girard-Egrot[1*]

[1]Institut de Chimie et Biochimie Moléculaires et Supramoléculaires, Université Lyon 1, University of Lyon, ICBMS, CNRS UMR 5246, Bât. Curien, 43 bd du 11 Nov. 1918, F-69622 Villeurbanne cedex, France
[2]Structural Chemistry Program, Eskitis Institute for Cell and Molecular Therapies, Griffith University, Brisbane, Qld 4111, Australia
[3]Faculty of Veterinary Science, The University of Melbourne, Parkville, Victoria, Australia

* To whom correspondence may be addressed: Pr. Agnès Girard-Egrot, Institut de Chimie et Biochimie Moléculaires et Supramoléculaires (ICBMS), Equipe GEMBAS, UMR CNRS 5246, Université Lyon 1, Bât Curien, 43 bd du 11 novembre 1918, 69622 Villeurbanne, FRANCE.
Tel: +33 4 72 44 85 32 ; Fax: +33 4 72 44 79 70
E-mail:agnes.girard-egrot@univ-lyon1.fr

Keywords: VIsinin-LIke Proteins (VILIPs), Neuronal Calcium Sensor (NCS) proteins, calcium-myristoyl switch, phosphoinositides, PIP_2, Langmuir monolayer, membrane model, brewster angle microscopy, protein-lipid interactions, interaction kinetic rate.

Abstract

VIsinin-LIke Proteins (VILIPs) are a subfamily of the Neuronal Calcium Sensor (NCS) proteins, which possess both N-myristoylation and EF-hand motifs allowing for a putative '*calcium-myristoyl switch*' regulation mechanism. It has previously been established that myristoyl conjugation increases the affinity of proteins for membranes, but, in many cases, a second feature such as a cluster of positively-charged residues is needed for stable membrane binding. The interaction of two members of this family, VILIP-1 and VILIP-3, with Langmuir monolayers as membrane models has been investigated in order to study the effects of both myristoylation and the highly basic region containing conserved poly-lysine residues on membrane association kinetics and binding properties. Results show that in the presence of calcium, N-myristoylation significantly increases the kinetic rate of VILIP adsorption to the membrane. Additionally, the proteins bind to negatively charged phospholipids independently of the conjugated myristate moiety. Besides the regulatory effect of calcium on the rate of binding presumably due to exposure of the myristoyl moiety ascribed to the '*calcium-myristoyl switch*', VILIP-1 and -3 also engage specific interactions with biomimetic membranes containing phosphatidylinositol 4,5-bisphosphate (PIP_2). The presence of PIP_2 increases the membrane association rates of both VILIPs. Taken together, these results show the major kinetic role of N-myristoylation for membrane binding, and highlight the critical role of specific phosphoinositide interactions for membrane association of members of the VILIP family.

1. Introduction

VIsinin-LIke Proteins (VILIPs) are myristoylated proteins belonging to the family of the Neuronal Calcium Sensor (NCS) proteins, and their membrane binding capacity is thought to be regulated by a '*calcium-myristoyl switch*' .

Lipid modifications of proteins play many roles inside and outside the cell . They facilitate membrane attachment of soluble proteins by enhancing interactions of proteins with either organelle or plasma membranes, occur in signaling and subcellular targeting by directing proteins to various cellular membranes, promote intra- and intermolecular protein-protein interactions, and may modulate protein structure and function .

N-myristoylation of proteins has been identified as an essential regulatory component of signal transduction networks in many eukaryote cells . It comprises the covalent attachment of the 14-carbon saturated fatty acid myristate to the N-terminal glycine through a stable amide bond. One of the major functions of this fatty acid acylation is to promote membrane binding of a wide variety of proteins by simple insertion of the hydrophobic myristate moiety into the lipid bilayer . The covalent attachment of myristate to a protein results in increased hydrophobicity of the protein, leading to higher membrane binding affinity . However, the increase in hydrophobicity is modest and often reversible membrane binding is observed. A central tenet, originally established by Peitzsch and McLaughlin , is that the effective dissociation constant K_d (approximately 10^{-4} M) of membrane-bound myristoylated peptides corresponds to an energy just enough for attachment of the peptides to the membrane. It is now an established paradigm that myristoylation, although necessary for membrane binding, is not sufficient to stably anchor a protein to a lipid bilayer .

Therefore, many myristoylated proteins require additional features for stable membrane binding, for example . an additional domain that interacts with another membrane-bound protein or a cluster of positively-charged residues often localized in the vicinity of the myristoylation site of the protein . Indeed, the N-terminal region of myristoylated proteins contains in many cases a polybasic region capable of electrostatic interactions with acidic phospholipid headgroups, mainly phosphatidylserine (PS) and phosphatidylinositol (PI) which, in healthy cells, are primarily localized to the inner leaflet of the bilayer, imparting a net negative charge to the cytoplasmic leaflet surface . In addition, the occurrence of a polybasic motif is now correlated with the targeting of plasma membrane proteins due to recognition of polyphosphoinositides, like $PI(3,4,5)P_3$ or $PI(4,5)P_2$, that are highly charged (valence of -4 at pH 7.0). Specific interactions with PIPs may target plasma membrane proteins to distinct cellular signaling processes .

When both myristate and polybasic motif are present within the protein, the hydrophobic and electrostatic forces synergize , but mechanistic details of this synergy have not been reported to date.

Functionally, protein lipid modifications can also act as reversible switches to activate or terminate signaling process. Indeed, the anchorage of *N*-myristoylated proteins to membranes may be dynamically regulated *via* various "myristoyl-switches". One of these switches relies on a "ligand"-dependent conformational change of the protein leading to exposure of the myristoyl moiety, previously sequestered in a hydrophobic pocket to outside, where it becomes available to participate in membrane binding. The switch can be triggered by binding of ligands or drugs, or by multimerization, thereby regulating the distribution of the myristoylated protein between cytosolic and membrane-bound states . This concept is exemplified the binding of calcium in the intramolecular '*calcium-myristoyl switch*' , where the transition of the conjugated myristoyl group from the buried to the exposed conformation is triggered by the binding of calcium cations to EF-hand motifs . Proteins that are subject to a

myristoyl switch typically exhibit a membrane binding regulation , but few mechanistic insights have been obtained to date.

The group of VIsinin-LIke Proteins (VILIPs) comprises of VILIP-1, VILIP-2, VILIP-3, hippocalcin and neurocalcin δ . These proteins are involved in many diseases such as Alzheimer's disease , schizophrenia and cancer . Previous studies have shown that VILIP-1 and VILIP-3 act at the membrane where they regulate the function of various membrane receptors like adenylate / guanylate cyclase, nicotinic acetylcholine receptor and natriuretic peptide receptor B . Cell biological studies have shown that VILIPs translocate to membranes upon stimulation by elevated intracellular calcium levels where they are implicated in signal transduction . However, at a molecular level, the mechanisms of membrane association are less clear. It has been established that members of the NCS family, including VILIPs, possess both an N-terminal myristoyl group and EF-hand structural motifs . The combination of these two structural elements is an essential component of the membrane binding regulation by the way of a '*calcium-myristoyl switch*' suggested for VILIPs , and first characterized in detail for recoverin, the prototypic member of the NCS family . . Intriguingly, the subcellular membrane localization of VILIPs differs substantially in living cells , and may be due to their capability to specifically bind to phosphatidyl inositides, most likely mediated through several highly conserved lysine residues in the N-terminal region of VILIPs . The existence of such a binding site has been supported by results from docking and molecular dynamics simulations . Nonetheless, the mechanistic interplay between protein-membrane electrostatic interactions and the membrane insertion of the myristoyl moiety in the presence of calcium during the membrane binding process is not fully understood.

In this work, we investigated the interaction of VILIP-1 and VILIP-3 with membrane models using Langmuir monolayers and Brewster Angle Microscopy (BAM). These techniques have been previously used to investigate the contribution of the myrsitoyl group and hydrophobic amino acids of recoverin to its binding dynamics . Recently, it has been employed to evaluate the effect of membrane composition in terms of charge and acyl chain saturation on the membrane binding of VILIPs, showing that the proteins initially interact with the membrane through electrostatic interactions . In the present study, we clearly show, by using myristoylated and unmyristoylated proteins, that the presence of calcium only increases the association kinetic rates of the myristoylated proteins with the membrane. We also demonstrate that membrane binding involves electrostatic interactions of the proteins with acidic phospholipid headgroups, and that the rate of binding is enhanced by the inclusion of PIP_2 into the membrane. We suggest that interactions of VILIPs with PIP_2, likely due to the presence of the polybasic region at the N-terminus, strengthens the association of VILIPs with the membrane and assists conformational changes in the protein triggered by the binding of calcium in the EF-hand sites, which accelerates the binding of VILIPs into membranes. These results reveal the major kinetic role of the N-myristoylation for the binding to the membrane, and highlight an important mechanistic role of phosphoinositides for membrane association of members of the VILIP family.

2. Material and methods

2.1 Chemicals

Ultrapure water was obtained from a PURELAB option Q7 system (VEOLIA WATER STI, France). Its resistivity and surface tension were 18.2 MΩ.cm and 72.8 mN/m at 20°C, respectively. 4-(2-Hydroxyethyl)-1-Piperazine ethane sulfonic acid (HEPES), sodium

chloride (NaCl), calcium chloride ($CaCl_2$) and Ethylenediamine tetra-acetic acid (EDTA) were purchased from Sigma (Saint-Quentin Fallavier, France). 1,2-dioleoyl-*sn*-glycero-3-phosphocholine (DOPC), 1,2-dioleoyl-*sn*-glycero-3-phosphoserine (DMPS), 1,2-dimyristoyl-*sn*-glycero-3-phosphocholine (DMPC),1,2-dimyristoyl-*sn*-glycero-3-phosphoserine (DMPS) and 1,2-dioleoyl-*sn*-glycero-3-phosphoinositol-4,5-bisphosphate ($PI(4,5)P_2$) were purchased from Avanti Polar Lipids (Alabaster, AL, USA). All chemicals were used as received. The phospholipid solutions were prepared in chloroform at a concentration of 1 mg/mL and stored at -20°C under argon to prevent lipid oxidation .

2.2 Preparation of recombinant VILIP-1 & VILIP-3

The recombinant wild-type proteins were produced as previously described . Briefly, VILIP-1 (ligated into pET8c) and VILIP-3 (ligated into pRSET_C) were expressed in BL21(DE3) cells, which in case of myristoylated VILIPs, were co-transformed with either of the above VILIP expression plasmids as well as N-myristoyl transferase (NMT; plasmid pBB131). Recombinant proteins were purified by subsequent anion exchange chromatography (QA52 column), and hydrophobic interaction chromatography, using a phenyl sepharose column. The purified proteins were stored in buffer containing 20 mM HEPES, 100 mM NaCl, pH 7.4, at a final concentration close to 1 mg/mL. Protein quality was monitored using denaturing SDS-PAGE and mass spectrometry.

2.3 Langmuir monolayer experiments

Monolayers were prepared using a homemade rectangular Langmuir PTFE-trough with a symmetrical compression system. The rectangular trough had a volume of 25 mL and a surface area of 49 cm². A Wilhelmy balance was used to measure the surface pressure (π), with an accuracy of ±0.5 mN/m. The trough was cleaned with successive baths of dichloromethane, ethanol and water, and filled with a filtered 20 mM HEPES buffer (pH 7.4), 150 mM NaCl, containing either 2 mM $CaCl_2$ or 2 mM EDTA. The subphase buffer was maintained at 20°C during all the experiments. Phospholipid mixture solutions in chloroform were gently spread at the air/liquid interface of the HEPES buffer subphase. After 15 minutes allowing solvent evaporation, the monolayer was compressed by the two mobile barriers until the desired surface pressures ranging from 5 to 20 mN/m and corresponding to the initial surface pressures (π_i). The protein was then injected into the subphase just beneath the lipid monolayer at a final concentration of 30 nM. The surface pressure variation induced by the interaction of the protein with the monolayer was continuously recorded as a function of time by using a computer-controlled Langmuir film balance (KSV NIMA) until the equilibrium surface pressure (π_e) was reached, indicating the end of the adsorption kinetics. All measurements were repeated at least three times for each condition and the average values were reported in this study.

2.4 Adsorption kinetics of VILIPs

The surface pressure increase ($\Delta\pi$ in mN/m) after injection of the proteins corresponded to π_e- π_i. The curves of surface pressure increase ($\Delta\pi$) as a function of time (t) recorded during the adsorption of VILIPs onto phospholipid monolayers corresponded to the adsorption kinetics of the protein. They were fitted using the stretched exponential equation adapted to surface pressure measurements by Pitcher *et al* , $\pi_t=\pi_e-\pi_i e^{-(kt)\beta}$ where π_t is the surface pressure of the monolayer at time t, π_e is the final equilibrium surface pressure after

protein adsorption, π_i is the initial surface pressure, *k* the rate coefficient of the binding of the protein onto the monolayer, and β is an exponential scaling factor.

2.5 Determination of the binding parameters of VILIPs

The different parameters that characterize the binding of VILIPs to different phospholipid membranes were determined as recently described . Briefly, the plot of the surface pressure increases ($\Delta\pi$) as a function of different initial surface pressures π_i allowed the determination of three different parameters: the Maximum Insertion Pressure (MIP) and the $\Delta\pi_0$ by extrapolating the regression of the plot to *x* and *y* axes, respectively; and the synergy factor (*a*) which is obtained by adding 1 to the slope of the plot of $\Delta\pi$ as a function of π_i . The uncertainty was determined as previously described . In this study, and because the parameter $\Delta\pi_0$ is more difficult to describe and still a point of debate , only MIP and (*a*) values will be presented.

2.6 Brewster Angle Microscopy

Brewster Angle Microscopy (BAM) allows the characterization of the lipid domain morphology of monolayers at the air/water interface . The phospholipid morphology before and after protein injection was determined using a Brewster angle microscope EP^3SW (Accurion, Germany) equipped with a 532 nm laser, a polarizer, an analyzer and a CCD camera. BAM image size was 483 x 383 µm.
For ultrathin films, the reflectance depends on both thickness and refractive index of the monolayer. Fitting reflectance data with BAM modeling software leads to a deduction of film thickness for a given refractive index . This model is based on the proportional relationship between the reflectance and the square of the interfacial film thickness when the optical index of the film is assumed constant . Since it was difficult to determine an accurate refractive index value under this condition, an average value of the refractive index, 1.46 for both lipid layers and proteins, was used in order to reduce the number of parameters introduced in the model . The different views of the interfacial film were reconstituted using BAM software EP^3viewer (Accurion, Germany) based on the brightness of the BAM pictures.

3. Results

To examine the role of the positively-charged region and N-myristoylation to the binding of VILIPs to membranes, we explored the membrane binding properties of four different proteins, VILIP-1 and VILIP-3 in their myristoylated and non-myristoylated forms, by using reconstituted monolayers at an air/liquid interface (Langmuir monolayers). Before characterization of binding, we investigated the interfacial behavior of each protein at the air/liquid interface in the absence of lipids in order to determine the optimal protein concentration to inject into the subphase for subsequent protein/lipid interaction analysis.

3.1 Adsorption of VILIPs at an air/liquid interface

Experiments without lipid at an air/liquid interface allow for the determination of: i) the tensio-active properties of the protein; ii) the concentration at which the protein saturates the lipid-free interface in order to minimize the protein aggregation that could result from a high protein concentration ; and iii) the concentration that will be used in the experiments with lipids. The protein concentration chosen based on these pre-evaluations is typically lower than the saturation concentration .

The adsorption of recombinant protein at varying subphase concentrations in the range of 3.75-30 nM was monitored by surface pressure measurements. At each concentration, the surface pressure equilibrated to a value indicating the end of the adsorption kinetics; this value indicates the equilibrium adsorption surface pressure (π_e). A typical relationship between π_e and the final protein concentration injected into the subphase containing 2 mM of $CaCl_2$ is shown in Figure 1A. For each protein, π_e values increased in a concentration dependent manner up to a saturation value. Depending on the individual protein, saturation levels were reached at a protein concentration of 15 or 30 nM (data not shown). At 30 nM, we found that myristoylated VILIP-1 and -3 possessed higher equilibrium adsorption surface pressures than the non-myristoylated proteins (Figure 1A– Inset).

After injection of myristoylated VILIP-1 and VILIP-3 into the subphase and equilibration of the surface pressure (π_e), BAM images were recorded in order to visualize the film homogeneity and to determine the estimated thickness of the protein monolayer from the calibrated reflectance values. These images (Figure 1B) revealed that at a concentration of 30 nM, proteins formed a homogeneous interfacial film without any aggregation, and that the estimated thickness of the protein monolayers was about 2.04 ± 0.21 nm and 2.34 ± 0.24 nm for myristoylated VILIP-1 and VILIP-3, respectively.

Since myristoylated VILIPs did not form aggregates under the chosen conditions, protein-lipid interactions can be investigated at 30 nM protein concentration at the lipid/liquid interface.

Figure 2 shows the adsorption kinetics of VILIP-1 in the presence or in the absence of calcium at the air-liquid interface at a final concentration of 30 nM. The difference in the adsorption surface pressure (π_e), although small, is significant. It could be ascribed to an increase in the hydrophobicity of the protein in the presence of calcium. Furthermore, the same adsorption surface pressure (π_e) was reached if calcium was absent from the subphase or if the myristoyl moiety was removed from the protein (non-myristoylated form). This result was in favor of a probable exposure of the myristoyl group due to the presence of calcium which arrests the protein at a naked air-liquid interface.

3.2 In the presence of calcium, N-myristoylation accelerates the binding of VILIPs to membranes

Next we investigated the membrane binding properties of myristoylated and unmyristoylated VILIP-1 and -3 to reconstituted monolayers at an air/liquid interface, in the presence or in the absence of calcium ions. Langmuir phospholipid monolayer films have become a standard model for studying lipid-protein interactions and they serve as mimics of biological membranes to study protein-membrane association . As electrostatic interactions are believed to be involved in the association of VILIPs to membranes , phospholipid monolayers composed of negatively charged (PS) and neutral lipids (PC) were used; both types of phospholipids are components of the inner leaflet of the plasma membrane.

The monolayers were compressed to an initial surface pressure (π_i) of 15 mN/m. Upon injection of protein into the subphase, the surface pressure variation ($\Delta\pi$ in mN/m) was recorded as a function of time, and the adsorption kinetics were fitted to the Pitcher's equation to determine the rate of binding *k* (Figure 3) . The final surface pressure variations ($\Delta\pi$ in mN/m) were independent of the presence or absence of calcium (Figure 3A). However, the maximum $\Delta\pi$ values were lower for the unmyristoylated compared to the myristoylated proteins. The absence or presence of calcium did not alter the kinetic curves for the unmyristoylated proteins, but caused slight differences for the myristoylated proteins.

The capacity of unmyristoylated proteins to interact with the biomimetic membrane indicates the existence of another binding site distinct from the conjugated lipid group.

Nevertheless, the highest final values of $\Delta\pi$ were obtained for the myristoylated proteins emphasizing the role of this lipo-conjugate in VILIP membrane association by either strengthening the protein binding to the membrane or anchoring more protein molecules to the membrane. Intriguingly, this effect elicited by the myristoyl group is independent of the presence of calcium since the same $\Delta\pi$ values were obtained with or without calcium for both myristoylated proteins at the end of the adsorption process (after ~50 minutes). The presence of calcium did not seem to affect the final affinity of VILIPs for membranes.

The second parameter characterizing monolayer adsorption kinetics is the rate of binding "*k"*. Determination of this parameter is possible by fitting the kinetic curve to the Pitcher's equation. It allows discrimination between different protein behaviors when similar $\Delta\pi$ values are observed .

In the case of VILIPs, a clear effect of calcium was observed on the rate of binding *k* of the myristoylated proteins (Figure 3B). In the presence of calcium, we observed an increase of 53% and 135% of the *k* value for myr-VILIP-1 and myr-VILIP-3 respectively, compared to the values obtained in the presence of EDTA. This effect was not observed for the unmyristoylated proteins. One explanation for these observations is that the mysistoyl moiety could be more rapidly available to interact with the monolayer in the presence of Ca^{2+}. Without N-myristoylation, calcium has no effect on the kinetics. Intriguingly, the values of *k* determined for myristoylated proteins in the absence of calcium were equal to those obtained for the unmyristoylated proteins in the presence or absence of calcium (Figure 3B). This suggests that binding involves another binding site, which is consistent with the existence of electrostatic interactions between VILIP-1 and -3 and the surface of membrane, as previously shown .

In summary, these results show that a part of the binding kinetics is independent of the presence of the myristoyl moiety. However, in the presence of calcium, it appears that the N-myristoylation accelerates binding of VILIPs to membranes. The kinetics is much faster than that of the non-myristoylated form. This last result is consistent with that previously reported for recoverin .

3.3 Effect of the myristoyl group on VILIP membrane binding properties

To further characterize the effects of the myristoyl group on the interaction of VILIPs with membranes, we monitored the surface pressure ($\Delta\pi$) after injection of the protein underneath the compressed monolayer with varying initial surface pressures (π_i) ranging from 5 to 20 mN/m (Figure 4). Such correlations are frequently analyzed to assess lipid-protein interactions and to distinguish electrostatic and hydrophobic interactions .

As shown in Figure 3A and B, the maximal insertion pressure (MIP) was significantly higher for myristoylated VILIP-1 and -3 than their unmyristoylated forms. In the presence of 2 mM $CaCl_2$, MIP values for VILIP-1 were 23.7 ± 2.8 mN/m and 18.6 ± 1.1 mN/m, respectively (Figure 4A). In the presence of 2 mM EDTA, MIP values were 22.7 ± 1.4 mN/m and 19.5 ± 1.5 mN/m. For myristoylated and unmyristoylated VILIP-3 (Figure 4B) MIP values of 26.6 ± 0.5 mN/m and 15.5 ±0.8 mN/m were obtained in presence of 2 mM $CaCl_2$. In the presence of 2 mM EDTA, MIP values were 24.4 ± 1.4 mN/m and 17.1 ± 3.4 mN/m. These results are in agreement with our previous conclusions on the role of N-myristoylation (see above). In the presence of calcium, the highest MIP values obtained for the myristoylated proteins demonstrate the membrane anchoring effect of the myristoyl group (Figure 3C). In contrast, removal of the myristate results in loss of membrane affinity. However, MIPs determined for both myristoylated proteins in the absence of calcium were similar to those obtained in the presence of the cation. Everything goes as if the calcium has no longer effect

on the extent of binding of the myristoylated proteins when these later are in interaction with the monolayer. The phenomenon was not observed in the absence of lipid at the air-liquid interface (Figure 2).

It has been previously shown by Salesse's group that the synergy factor "*a*" can deliver insights into mechanisms governing protein binding to lipid monolayers. A positive *a* value indicates favorable conditions for protein monolayer binding. A synergy factor of zero corresponds to a stationary state, without any favored or disfavored protein membrane binding. Finally, a negative synergy factor indicates repulsion between the protein and the monolayer. Here, our data yield synergy factors with substantially positive values for myristoylated proteins ($a = 0.522 \pm 0.059$ for myr-VILIP-1 and 0.312 ± 0.007 for myr-VILIP-3), and around zero for the unmyristoylated proteins (Figure 4D). These values agree with the notion that the presence of the myristoyl group facilitates the association of VILIPs to the monolayer. In the absence of N-myristolyation, the membrane binding properties of VILIPs are markedly less sensitive to the physical state of the lipid in the monolayer. The synergy factor is also a measure of the sensitivity for the packing of phospholipid acyl chains. The insertion of the myristoyl group within the monolayer is favored by the hydrophobic chain organization. Membrane binding becomes insensitive to the acyl chain organization when it is only mediated by surface electrostatic interactions.

3.4 VILIPs bind to negatively charged phospholipids

In order to assess the potential organizational changes within the monolayer upon lipid/protein interactions, Brewster angle microscopy (BAM) was used to scrutinize the morphologies of phospholipid monolayers. As shown in Figure 5 (top line), DOPC/DOPS (1:3) monolayers were homogenous irrespective of the surface pressures applied. From the BAM calibration procedure and thickness model , we determined by using the true reflectance value an average thickness of 1.3 nm for pure lipid monolayers compressed at 15 or 25 mN/m, respectively, consistent with the thickness of one membrane leaflet in a fluid phase (Table 1). After injection of myristoylated VILIPs beneath monolayers compressed at π_i of 15 mN/m, and subsequent equilibration (π_e = 21 mN/m for myr-VILIP-1 and 25 mN/m for VILIP-3), the monolayers remained homogeneous (Fig. 4 - top line). The global thickness of the film increased from 1.30 to 1.98 nm for myr-VILIP1, and from 1.30 to 2.32 nm for myr-VILIP-3, due to the interaction of these proteins with the fluid monolayer. The phase transition temperature of phospholipids can affect the occurrence of morphological changes in the membrane. Since 1,2-dioleyl-*sn*-glycero-3-phospholipids (DOPC and DOPS) remained in the fluid phase in the experimental conditions used in this study, we also tested 1,2-dimyristoyl-*sn*-glycero-3-phospholipids, DMPC and DMPS, which possess different phase transition temperatures to examine the effect of phospholipid reorganization on membrane binding . In the absence of protein, DMPC/DMPS (1:3) monolayers exhibited a classical phase segregation mediated by the presence of calcium in the subphase: the negatively-charged phospholipids DMPS segregated into condensed domains (bright clusters), whilst DMPC remained in the fluid phase (dark background) (Fig 4 – bottom line). The average thickness of each phase was 2.15 nm and 1.62 nm, respectively, consistent with those expected for a condensed or a fluid phase (Table 1). In the presence of myristoylated VILIPs at equilibrium surface pressure, a drastic modification of the monolayer morphology was observed with a large rearrangement of the phospholipid organization compared to the pure monolayers at similar surface pressures. Although no significant change was detected in the estimated thicknesses upon injection (Table 1), in the condensed phase of DMPC/DMPS (1:3) bright dots appeared in the BAM images, especially in the presence of myr-VILIP-3 (Fig 4 –

Inset - red arrows). The film thickness in the area of these bright dots was determined to ~3 nm for both myristoylated VILIPs (Table 1). Although this thickness does not correspond to the sum of monolayer and protein thicknesses, one can assume that VILIPs may preferentially interact with the negatively charged condensed domains of PS. In line with this assumption are the results obtained with unmyristoylated VILIPs in this experiment (Figure 5 and Table 1) which show the same membrane reorganization and estimated thicknesses.

Clearly, these effects are independent of the myristoylation state and thus due to other interactions between VILIPs and the membrane. The BAM images suggest that VILIPs bind to the negatively charged phospholipids, suggesting that the basic residues in the N-terminal region of the proteins is involved in the association process.

3.5 Phosphoinositides enhance membrane interaction of VILIPs

It has been suggested that VILIPs can bind to phosphoinositol derivatives such as $PI(4,5)P_2$. In order to investigate potential effects of phosphoinositides on the adsorption kinetics of VILIPs, we conducted time-dependent adsorption experiments to DMPC/DMPS (1:3) monolayers containing 1% PIP_2 while maintaining a constant net negative charge on the monolayer surface. The exact composition of the monolayer was thus DMPC 25%, DMPS 74%, PIP_2 1%. No particular change was observed either for the morphology (Figure 6A) or the estimated thickness (data not shown) of the films in the presence of myristoylated VILIPs when compared to a DMPC/DMPS (1:3) monolayer without proteins. Similarly, no major differences were observed at the end of the adsorption process: PIP_2 did not induce significant variations of the final surface pressure increase ($\Delta\pi$ values) upon VILIPs interaction (Figure 6B). In constrast, a significant effect was observed for the values of the rate of binding *k* (Figure6C). Despite the net negative charge being the same in the monolayers with and without 1% PIP_2, the binding rate of all proteins was significantly increased in the presence of PIP_2 (30% increase in the case of the myristoylated proteins).

These results agree with the suggestion that VILIPs can interact specifically with phosphoinositides and demonstrate that the main effect of PIP-containing membranes is of a kinetic nature. Again, since this increase was observed for myristoylated and unmyristoylated proteins in this study, we can assume that this specific interaction is independent of lipo-conjugation of VILIPs and most likely localizes to the binding site identified in previous modelling/molecular dynamics experiments . It is consistent with the fact that any protein with a cluster of four or more basic residues located at the membrane-solution interface should laterally sequester PIP_2 . Importantly, specific interactions of VILIPs with PIPs support the notion of PIP-targeting by VILIPs as a way to regulate its subcellular location.

4. Discussion

VILIPs have been implied in signal transduction processes , since they translocate to the plasma membrane following a stimulus that provides elevated intracellular calcium concentration. This translocation is thought to rely on an intramolecular '*calcium-myristoyl switch*'. Moreover, a putative basic cluster of conserved poly-lysine residues in the N-terminal region of *N*-myristoylated VILIPs could provide a potential site for binding specifically phosphoinositides, and more precisely PIP_2 , and thus provide a moelcular mechanism for the different subcellular localizations of VILIPs in the living cells . As mentioned in the introduction, the two-signal model '*Myristate plus Basic*' is well known to mediate efficient membrane binding. .

In this study, we have investigated the membrane binding properties of VILIP-1 and VILIP-3 by using Langmuir monolayers as membrane models which offer the possibility to analyze in detail the membrane binding kinetics. The choice of this system was based on its simple experimental design and its compatibility with monotopic protein insertion in the membrane. By using a set of myristoylated and non-myristoylated proteins, we demonstrated that a part of the kinetics of binding to PS-containing lipid monolayers is controlled by the electrostatic interactions. Interestingly, the rate of binding *k* is of the same order of magnitude for mutated proteins (with or without calcium) and myristoylated proteins in the absence of calcium, for which the myristoyl group is supposed to be buried. This result suggests that the interactions between VILIPs and negatively charged membranes involve other structural features aside from the myristate. Similar results have previously been obtained for the NADH-cytochrome b5 reductase, where the association with the membrane of the non-myristoylated form of the enzyme was not different from that of the natural, myristoylated form . These interactions are most likely of electrostatic nature and presumably mediated by the conserved basic residues found on the surface of VILIPs in the N-terminal region .

In the presence of calcium, the association of myristoylated forms is markedly accelerated (highest *k* values), but at the end, the same final organization is reached (same $\Delta\pi$ values obtained for wild-type proteins in the presence or not of Ca^{2+}, Figure 3). The presence of calcium affects the kinetics of binding of the proteins but not the final affinity. Again, this result presents a striking similarity with the finding of Strittmatter *et al*. who reported that the effect of N-myristoylation appears to be restricted to facilitate and stabilize the interaction of the cytochrome b5 reductase NADH with phospholipid vesicles .

Even in the absence of calcium, it appears as if the myristoyl group is extracted from its protein-buried location and inserts into the monolayer. This phenomenon is not observed if the lipids are not present at the air-liquid interface; on the contrary, the kinetics are not changed and the equilibrium surface pressure π_e is higher for the *N*-myristoylated proteins in the presence of calcium (Figure 2).

Altogether, this result highlights the synergy of the electrostatic interactions and the N-myristoylation in the presence of calcium for VILIP binding to membranes. As previously shown , the electrostatic interactions are probably responsible for the very first interactions of the protein with the membrane. Once associated to the membrane, we could assume that some conformational changes must operate to finally ensure the ejection of the myristoyl moiety from its hydrophobic pocket and anchor the protein on the membrane, thus leading to no apparent change in the final affinity of *N*-myristoylated proteins. In the presence of calcium, the ejection is triggered and the insertion of the myristate within the membrane is faster, which only impacts the adsorption kinetics of the *N*-myristoylated proteins (not the final membrane-bound state). This kinetic role is consistent with the function of the *N*-myristoylated proteins regulated by a '*calcium-myristoyl switch*' in the activation (or termination) of signaling process. Since in the absence of electrostatic interactions (interface without lipid) the myristoyl group does not eject if calcium is not present (Figure 2), it may be also assumed that the electrostatic interactions prefigure the rapid conformational changes triggered by the calcium binding.

The analysis of the influence of the lipid packing on VILIP- membrane interaction has shown that *N*-myristoylated proteins exhibit a higher affinity than unmyristoylated forms as shown by the higher MIPs (Figure 4). This result is consistent with the two-signal model '*Myristate plus Basic*' in which the hydrophobic and electrostatic forces synergize to mediate efficient membrane binding: the positively charged residues associate electrostatically with acidic phospholipids to stabilize membrane binding, while myristate provides membrane-

binding energy *via* hydrophobic interactions, giving a greater binding ability to the wild-type proteins . As revealed by the analysis of the synergy factor, the insertion of the myristoyl moiety within the monolayer is favored by the packing of the phospholipid acyl chains. (Membrane binding becomes insensitive to the acyl chain organization when it is only mediated by electrostatic interactions). Adding a myristate confers a relatively small hydrophobicity to the protein because this saturated acyl chain is short. If the penetration of the myristate into the membrane is favored by the packing chain, it is probably because the hydrophobic interactions are more stronger in a more condensed monolayer and this has to consequence to stabilize the myristate moiety in the membrane after insertion (approximately 10 of the 14 carbons penetrate the hydrocarbon core of bilayer). This point may be correlated to the possible targeting of lipid-modified proteins to plasma membrane nanodomains, when a second acylation occurs.

BAM analysis of the morphology changes of a mixed monolayer of DMPC/DMPS (1:3) segregated by the presence of calcium in the subphase upon interaction of both *N*-myristoylated and non-myristoylated forms of VILIPs has clearly evidenced that VILIPs interact more specifically with phosphatidylserine (PS) (red arrows, Figure 5). This result confirms that VILIPs can interact with acidic phospholipid headgroups. This interaction could be mediated by the conserved polybasic residues in the N-terminus . But, more interesting is the specific effect of PIP_2 on the membrane binding of VILIPs. Adding only 1% of PIP_2 – which corresponds to the percentage of this phosphoinositide in the cytoplasmic leaflet of the plasma membrane – to DMPC/DMPS mixture whilst maintaining constant the negative charge amount in the monolayer provokes an increase of the binding kinetics rate of all myristoylated and unmyristoylated proteins (higher rates of binding *k*, Figure 6) without changing their final membrane-bound states (same $\Delta\pi$ values, Figure 6). This phenomenon is probably the result of specific electrostatic interactions between the conserved polybasic domain and the highly charged PIP_2 headgroup which reinforces the association of VILIPs to the membrane. In the case of *N*-myristoylated proteins, we can assume that this tightening may assist the conformational changes triggered by the calcium binding. This effect agrees with a PIP-dependent targeting mechanism that directs VILIPs to particular subcellular localizations where it can promote distinct cellular processes .

In conclusion, all results obtained in this present report highlight the distinct role of electrostatic interactions, which could be mediated by the polybasic domain in the N-terminal region of VILIPs, and interaction of the myristoyl moiety with the membrane, which could be triggered by calcium binding. We propose that the electrostatic interactions would be responsible for the very first interactions of the protein with the membrane, and the ejection of the myristoyl group would have only an impact on the adsorption kineticrates of the *N*-myristoylated proteins. Additionally, membrane interactions solely mediated by electrostatic interactions would also lead to an ejection of the myristoyl moiety. In view of our results, we could assume that electrostatic interactions help to the efficiency of the calcium binding to the protein by inducing subtle conformational changes that would assist the binding of calcium that triggers the release of the myristoyl group. This point seems to be exemplified by the specific interactions with PIP_2. The specific electrostatic interactions with PIP_2would be not simply requested for the first step of the membrane targeting: it would contributealso to an accelerated membrane binding process.This kinetic effect is consistent with the activation of subcellular signaling processes mediated by the specific interactions with PIPsof proteins which are addressed to the plasma membranewhere they regulate the function of various membrane receptors.

Acknowledgements

We thank Jeffery Gordon (Washington University St-Louis) for sharing the pNMT expression plasmid pBB131, and Karl-Heinz Braunewell for providing the cDNA of VILIP-1 and VILIP-3. We thank Christian Salesse for helpful discussions. Conan K. Wang was supported by a National Health and Medical Research Council Early Career Fellowship (546578). Samuel Rebaud was supported by a French Ministry of Science and Education fellowship. This work was supported in parts by FundacaoBial and the Rebecca Cooper Foundation (to Andreas Hofmann).

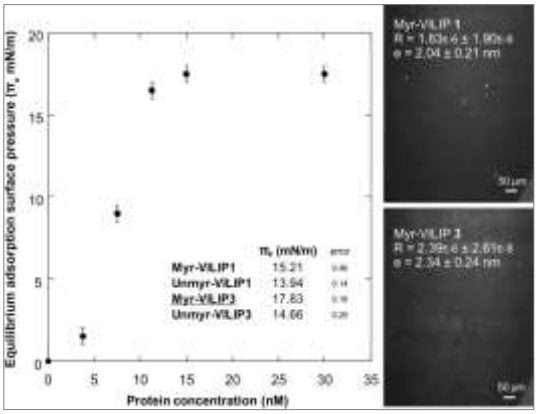

Figure 1 : Adsorption of protein at an air/liquid interface. (**A**) Typical curve of the equilibrium adsorption surface pressure (π_e) reached at the end of the adsorption kinetics for different protein concentration injected into the subphase. Each point corresponds to the mean value of three kinetic experiments. (**Inset**) Values of (π_e) for each protein at 30 nM. (**B**) BAM images at equilibrium surface pressure after injection of myr-VILIP1 or myr-VILIP3 at a final concentration of 30 nM, with corresponding reflectance and estimated thickness for a reflective index value of 1.46. Subphase : 20 mM HEPES 150 mM NaCl 2mM $CaCl_2$

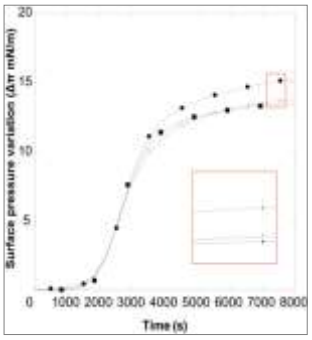

Figure 2. Adsorption kinetics of VILIPs in the presence or in the absence of calcium at the air-liquid interface for a final concentration of 30 nM. Representative surface pressure variation as a function of time for myristoylated (circle) or unmyristoylated (square) VILIP-1 injected into the buffer. The curves render during adsorption of the protein at the air-liquid interface in the presence of 2 mM $CaCl_2$ (black) or 2 mM EDTA (white).

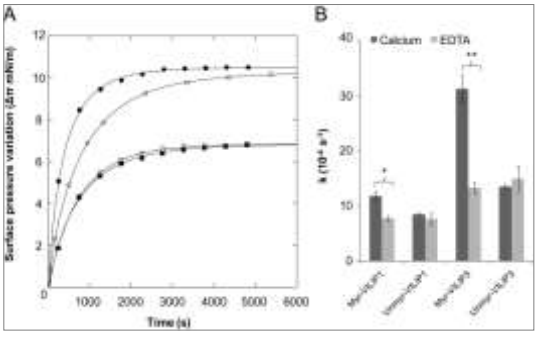

Figure 3. Adsorption kinetics of VILIPs onto DOPC/DOPS (1:3) phospholipid monolayers. (A) Representative surface pressure variation as a function of time for myristoylated (circle) or unmyristoylated (square) VILIP-3 injected underneath the monolayer initially compressed at an initial surface pressure (π_i) of 15 mN/m. The curves render during adsorption of the protein in the presence of 2 mM $CaCl_2$ (black) or 2 mM EDTA (white). All kinetics are fitted to the Pitcher's equation which allowed the determination of the rate of binding (***k***). The same variation profil has been obtained with VILIP-1. (**B**) Rate of binding for VILIP-1 and VILIP-3 (***** $p < 0,05$; ****** $p < 0,01$).

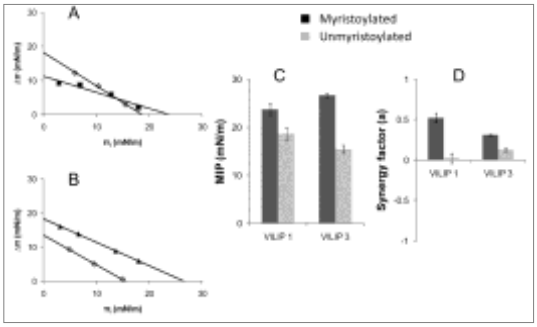

Figure 4. Determination of the maximal insertion pressure (MIP) and synergy factor (*a*) of VILIPs. (Left) Plot of the surface pressure increase ($\Delta\pi$) as a function of the initial surface pressure (π_i) to determine the MIP and the synergy factor (*a*) for myristoylated (square) and unmyristoylated (circle) VILIP-1 (**A**) and for myristoylated (triangle) and unmyristoylated (diamond) VILIP-3 **(B)** in interaction with a DOPC/DOPS (3:1) phospholipid monolayer. The subphase was supplemented by 2 mM $CaCl_2$. (**Right**) Histograms of MIP**(C)** and synergy factor (*a*) **(D)** for VILIPs in the presence of calcium. Same results and effects have been obtained in the absence of calcium (data not shown).

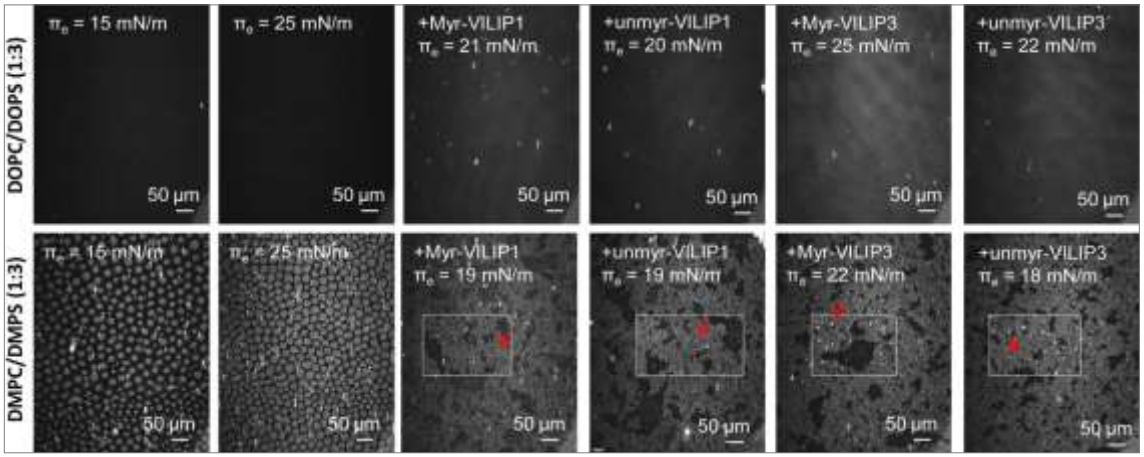

Figure 5. Effects of the VILIPs adsorption on the lipid monolayer morphology. Interface visualization using Brewster angle microscopy of DOPC/DOPS (1:3) (**Top Line**) or DMPC/DMPS (1:3) (**Bottom Line**) monolayer at 15 mN/m or 25 mN/m, and at π_0 after injection of notified VILIPs (π_i = 15mN/m). Red arrows indicated bright dots in condensed phase.

		Thickness (nm) - *Reflectance*					
Lipids composition	Phase	Lipid Monolayer		Lipid Monolayer in interaction with			
		15 mN/m	**25** mN/m	**Myr-VILIP1**	**unmyr-VILIP1**	**Myr-VILIP3**	**unmyr-VILIP3**
DOPC/DOPS (1:3)	Fluid	1.30 ± 0.11 *0.74e^{-7} ± 0.56e^{-8}*	1.33 ± 0.11 *0.77e^{-7} ± 0.57e^{-8}*	1.98 ± 0.20 *1.72e^{-8} ± 1.77e^{-8}*	1.75 ± 0.17 *1.35e^{-7} ± 1.30e^{-8}*	2.32 ± 0.24 *2.35e^{-7} ± 2.62e^{-8}*	1.75 ± 0.16 *1.34e^{-7} ± 1.15e^{-8}*
DMPC/DMPS (1:3)	Fluid	1.64 ± 0.15 *1.18e^{-6} ± 0.93e^{-8}*	1.62 ± 0.15 *1.15e^{-7} ± 0.92e^{-8}*	1.66 ± 0.15 *1.21e^{-7} ± 1.00e^{-8}*	1.53 ± 0.14 *1.03e^{-7} ± 0.82e^{-8}*	1.64 ± 0.15 *1.18e^{-7} ± 0.98e^{-8}*	1.63 ± 0.15 *1.16e^{-7} ± 0.95e^{-8}*
	Condensed	2.16 ± 0.20 *2.05e^{-7} ± 1.72e^{-8}*	2.15 ± 0.22 *2.02e^{-7} ± 2.22e^{-8}*	2.12 ± 0.21 *1.97e^{-7} ± 1.91e^{-8}*	2.29 ± 0.23 *2.29e^{-7} ± 2.44e^{-8}*	2.23 ± 0.22 *2.17e^{-7} ± 2.31e^{-8}*	2.26 ± 0.21 *2.24e^{-7} ± 1.90e^{-8}*
	Bright Dots (Condensed)			**2.87** ± 0.27 *3.61e^{-8} ± 3.26e^{-8}*	**3.04** ± 0.30 *4.06e^{-7} ± 3.91e^{-8}*	**3.00** ± 0.28 *3.94e^{-7} ± 3.42e^{-8}*	**3.06** ± 0.23 *4.10e^{-7} ± 2.44e^{-8}*

Table 1. Estimated Thicknesses and reflectance values of the film present at air buffer interface. Thickness values were estimated using the reflectance value, for a refractive index value of 1.46.

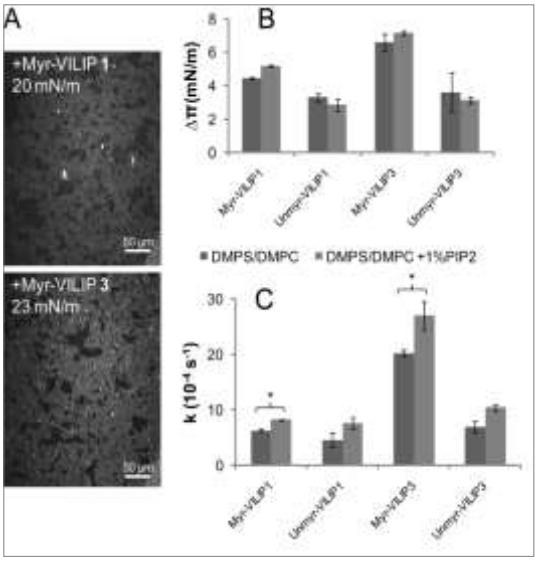

Figure 6. Influence of PIP_2 on VILIPs membrane binding properties. (A) Interface visualization using Brewster angle microscopy of DMPC/DMPS (1:3) containing 1% PIP_2 at negative constant charge. **(B)** Surface pressure increase (ΔΠ) upon interaction of VILIPs injected under DMPC/DMPS (1:3) ± 1%PIP_2 monolayers in the presence of 2 mM calcium. **(C)** Rate of binding determined in the same experimental conditions (* $p < 0,02$).

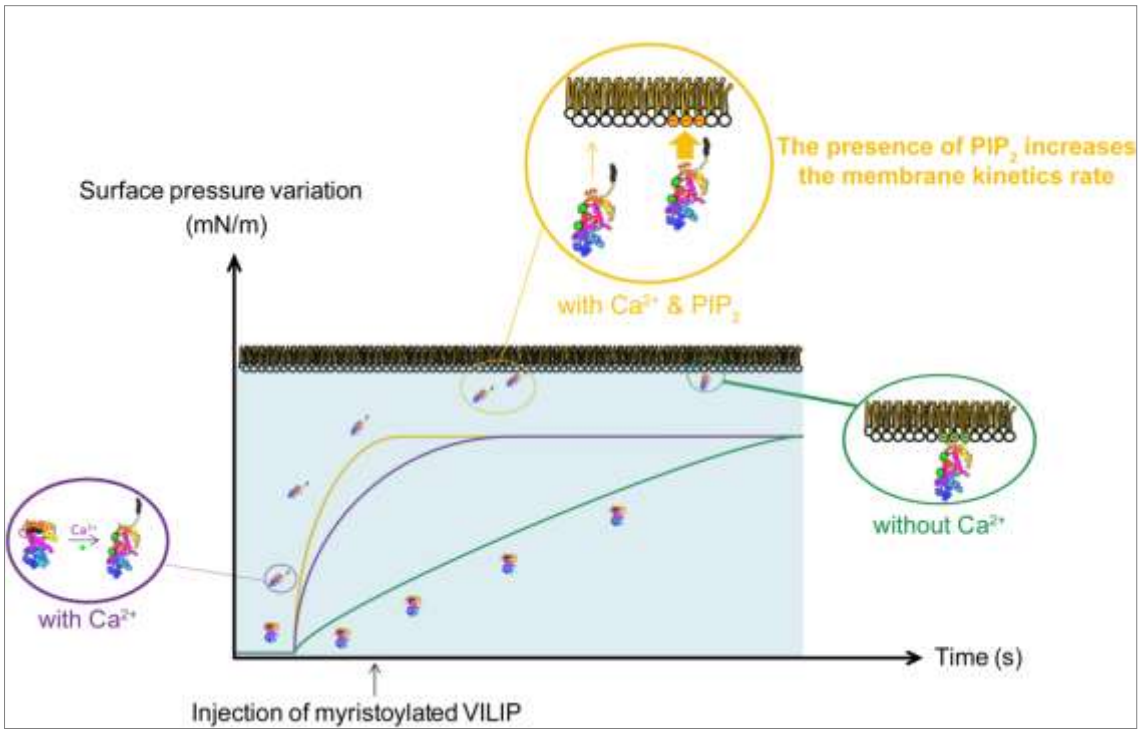

References

[1] C. Spilker, T. Dresbach, K.H. Braunewell, Reversible translocation and activity-dependent localization of the calcium-myristoyl switch protein VILIP-1 to different membrane compartments in living hippocampal neurons, The Journal of Neuroscience, 22 (2002) 7331-7339.
[2] C. Spilker, K.H. Braunewell, Calcium-myristoyl switch, subcellular localization, and calcium-dependent translocation of the neuronal calcium sensor protein VILIP-3, and comparison with VILIP-1 in hippocampal neurons, Mol Cell Neurosci, 24 (2003) 766-778.
[3] S. Maurer-Stroh, B. Eisenhaber, F. Eisenhaber, N-terminal N-myristoylation of proteins: refinement of the sequence motif and its taxon-specific differences, Journal of Molecular Biology, 317 (2002) 523-540.
[4] T. Chida, M. Ando, T. Matsuki, Y. Masu, Y. Nagaura, T. Takano-Yamamoto, S. Tamura, T. Kobayashi, N-Myristoylation is essential for protein phosphatases PPM1A and PPM1B to dephosphorylate their physiological substrates in cells, Biochemical Journal, 449 (2013) 741-749.
[5] D.D.O. Martin, E. Beauchamp, L.G. Berthiaume, Post-translational myristoylation: Fat matters in cellular life and death, Biochimie, 93 (2011) 18-31.
[6] M.D. Resh, Trafficking and signaling by fatty-acylated and prenylated proteins, Nat Chem Biol, 2 (2006) 584-590.
[7] M.D. Resh, Targeting protein lipidation in disease, Trends in Molecular Medicine, 18 (2012) 206-214.
[8] M.D. Resh, Covalent lipid modifications of proteins, Current Biology, 23 (2013) R431-R435.
[9] H. Ezanno, E. Beauchamp, F. Lemarié, P. Legrand, V. Rioux, L'acylation des protéines : une fonction cellulaire importante des acides gras saturés, Nutrition Clinique et Métabolisme, 27 (2013) 10-19.
[10] N. Sorek, D. Bloch, S. Yalovsky, Protein lipid modifications in signaling and subcellular targeting, Current Opinion in Plant Biology, 12 (2009) 714-720.
[11] J.A. Traverso, C. Micalella, A. Martinez, S.C. Brown, B. Satiat-Jeunemaître, T. Meinnel, C. Giglione, Roles of N-Terminal Fatty Acid Acylations in Membrane Compartment Partitioning: Arabidopsis h-Type Thioredoxins as a Case Study, The Plant Cell Online, 25 (2013) 1056-1077.
[12] M. Wright, W. Heal, D. Mann, E. Tate, Protein myristoylation in health and disease, J Chem Biol, 3 (2010) 19-35.
[13] M.D. Resh, Fatty acylation of proteins: new insights into membrane targeting of myristoylated and palmitoylated proteins, Biochimica et Biophysica Acta (BBA) - Molecular Cell Research, 1451 (1999) 1-16.
[14] S. Maurer-Stroh, F. Eisenhaber, Myristoylation of viral and bacterial proteins, Trends in Microbiology, 12 (2004) 178-185.
[15] R.M. Peitzsch, S. McLaughlin, Binding of acylated peptides and fatty acids to phospholipid vesicles: Pertinence to myristoylated proteins, Biochemistry, 32 (1993) 10436-10443.
[16] M. Resh, Membrane Targeting of Lipid Modified Signal Transduction Proteins, in: P. Quinn (Ed.) Membrane Dynamics and Domains, vol. 37, Springer US, 2004, pp. 217-232.
[17] J.B. McCabe, L.G. Berthiaume, Functional Roles for Fatty Acylated Amino-terminal Domains in Subcellular Localization, Molecular Biology of the Cell, 10 (1999) 3771-3786.
[18] R. Tarawneh, G. D'Angelo, E. Macy, C. Xiong, D. Carter, N.J. Cairns, A.M. Fagan, D. Head, M.A. Mintun, J.H. Ladenson, J.M. Lee, J.C. Morris, D.M. Holtzman, Visinin-like protein-1: diagnostic and prognostic biomarker in Alzheimer disease, Annals of neurology, 70 (2011) 274-285.
[19] L.J. Parent, C.B. Wilson, M.D. Resh, J.W. Wills, Evidence for a second function of the MA sequence in the Rous sarcoma virus Gag protein, Journal of Virology, 70 (1996) 1016-1026.
[20] M.P. Czech, PIP2 and PIP3, Cell, 100 (2000) 603-606.
[21] W.D. Heo, T. Inoue, W.S. Park, M.L. Kim, B.O. Park, T.J. Wandless, T. Meyer, PI(3,4,5)P3 and PI(4,5)P2 Lipids Target Proteins with Polybasic Clusters to the Plasma Membrane, Science, 314 (2006) 1458-1461.
[22] J.B. Ames, T. Tanaka, L. Stryer, M. Ikura, Portrait of a myristoyl switch protein, Current Opinion in Structural Biology, 6 (1996) 432-438.
[23] J.B. Ames, R. Ishima, T. Tanaka, J.I. Gordon, L. Stryer, M. Ikura, Molecular mechanics of calcium-myristoyl switches, Nature, 389 (1997) 198-202.
[24] S. McLaughlin, A. Aderem, The myristoyl-electrostatic switch: a modulator of reversible protein-membrane interactions, Trends in Biochemical Sciences, 20 (1995) 272-276.
[25] K.H. Braunewell, A.J. Klein-Szanto, Visinin-like proteins (VSNLs): interaction partners and emerging functions in signal transduction of a subfamily of neuronal Ca2+ -sensor proteins, Cell and tissue research, 335 (2009) 301-316.
[26] J.F. Loring, X. Wen, J.M. Lee, J. Seilhamer, R. Somogyi, A gene expression profile of Alzheimer's disease, DNA Cell Biol, 20 (2001) 683-695.

[27] X. Luo, L. Hou, H. Shi, X. Zhong, Y. Zhang, D. Zheng, Y. Tan, G. Hu, N. Mu, J. Chan, X. Chen, Y. Fang, F. Wu, H. He, Y. Ning, CSF levels of the neuronal injury biomarker visinin-like protein-1 in Alzheimer's disease and dementia with Lewy bodies, Journal of neurochemistry, (2013).
[28] H.-G. Bernstein, K.-H. Braunewell, C. Spilker, P. Danos, B. Baumann, S. Funke, S. Diekmann, E.D. Gundelfinger, B. Bogerts, Hippocampal expression of the calcium sensor protein visinin-like protein-1 in schizophrenia, NeuroReport, 13 (2002) 393-396.
[29] P. Gierke, C. Zhao, H.G. Bernstein, C. Noack, R. Anand, U. Heinemann, K.H. Braunewell, Implication of neuronal Ca2+ -sensor protein VILIP-1 in the glutamate hypothesis of schizophrenia, Neurobiology of disease, 32 (2008) 162-175.
[30] H. Mahloogi, A.M. Gonzalez-Guerrico, R. Lopez De Cicco, D.E. Bassi, T. Goodrow, K.H. Braunewell, A.J. Klein-Szanto, Overexpression of the calcium sensor visinin-like protein-1 leads to a cAMP-mediated decrease of in vivo and in vitro growth and invasiveness of squamous cell carcinoma cells, Cancer Res, 63 (2003) 4997-5004.
[31] J. Fu, K. Fong, A. Bellacosa, E. Ross, S. Apostolou, D.E. Bassi, F. Jin, J. Zhang, P. Cairns, I. Ibanez de Caceres, K.H. Braunewell, A.J. Klein-Szanto, VILIP-1 downregulation in non-small cell lung carcinomas: mechanisms and prediction of survival, PloS one, 3 (2008) e1698.
[32] M. Liu, H. Yang, D. Fang, J.J. Yang, J. Cai, Y. Wan, D.H. Chui, J.S. Han, G.G. Xing, Upregulation of P2X3 receptors by neuronal calcium sensor protein VILIP-1 in dorsal root ganglions contributes to the bone cancer pain in rats, Pain, (2013).
[33] F.F. Dai, Y. Zhang, Y. Kang, Q. Wang, H.Y. Gaisano, K.H. Braunewell, C.B. Chan, M.B. Wheeler, The neuronal Ca2+ sensor protein visinin-like protein-1 is expressed in pancreatic islets and regulates insulin secretion, The Journal of biological chemistry, 281 (2006) 21942-21953.
[34] C.J. Zhao, C. Noack, M. Brackmann, T. Gloveli, A. Maelicke, U. Heinemann, R. Anand, K.H. Braunewell, Neuronal Ca2+ sensor VILIP-1 leads to the upregulation of functional alpha4beta2 nicotinic acetylcholine receptors in hippocampal neurons, Mol Cell Neurosci, 40 (2009) 280-292.
[35] J. Buttgereit, F. Qadri, J. Monti, T.H. Langenickel, R. Dietz, K.H. Braunewell, M. Bader, Visinin-like protein 1 regulates natriuretic peptide receptor B in the heart, Regulatory peptides, 161 (2010) 51-57.
[36] C. Spilker, E.D. Gundelfinger, K.H. Braunewell, Evidence for different functional properties of the neuronal calcium sensor proteins VILIP-1 and VILIP-3: from subcellular localization to cellular function, Biochim Biophys Acta, 4 (2002) 1-2.
[37] C.K. Wang, A. Simon, C.M. Jessen, C.L.P. Oliveira, L. Mack, K.-H. Braunewell, J.B. Ames, J.S. Pedersen, A. Hofmann, Divalent Cations and Redox Conditions Regulate the Molecular Structure and Function of Visinin-Like Protein-1, PloS one, 6 (2011) e26793.
[38] K.C. Chen, L.K. Wang, L.S. Chang, Regulatory elements and functional implication for the formation of dimeric visinin-like protein-1, Journal of peptide science : an official publication of the European Peptide Society, 15 (2009) 89-94.
[39] K. Braunewell, B. Paul, W. Altarche-Xifro, C. Noack, K. Lange, A. Hofmann, Interactions of Visinin-like Proteins with Phospho-inositides, Australian Journal of Chemistry, 63 (2010) 350-356.
[40] J. Boucher, E. Trudel, M. Méthot, P. Desmeules, C. Salesse, Organization, structure and activity of proteins in monolayers, Colloids and Surfaces B: Biointerfaces, 58 (2007) 73-90.
[41] P. Desmeules, S.-É. Penney, B. Desbat, C. Salesse, Determination of the Contribution of the Myristoyl Group and Hydrophobic Amino Acids of Recoverin on its Dynamics of Binding to Lipid Monolayers, Biophysical Journal, 932069-2082.
[42] S. Rebaud, A. Simon, C.K. Wang, L. Mason, L. Blum, A. Hofmann, A. Girard-Egrot, Comparison of VILIP-1 and VILIP-3 Binding to Phospholipid Monolayers, PloS one, 9 (2014) e93948.
[43] E. Boisselier, P. Calvez, E. Demers, L. Cantin, C. Salesse, Effect of oxidation of polyunsaturated phospholipids on the binding of proteins in monolayers, Colloids and surfaces. B, Biointerfaces, 109 (2013) 109-114.
[44] J.A. Cox, I. Durussel, M. Comte, S. Nef, P. Nef, S.E. Lenz, E.D. Gundelfinger, Cation binding and conformational changes in VILIP and NCS-1, two neuron-specific calcium-binding proteins, Journal of Biological Chemistry, 269 (1994) 32807-32813.
[45] W.H. Pitcher Iii, S.L. Keller, W.H. Huestis, Interaction of nominally soluble proteins with phospholipid monolayers at the air–water interface, Biochimica et Biophysica Acta (BBA) - Biomembranes, 1564 (2002) 107-113.
[46] P. Calvez, E. Demers, E. Boisselier, C. Salesse, Analysis of the contribution of saturated and polyunsaturated phospholipid monolayers to the binding of proteins, Langmuir : the ACS journal of surfaces and colloids, 27 (2011) 1373-1379.
[47] É. Boisselier, P. Calvez, É. Demers, L. Cantin, C. Salesse, Influence of the Physical State of Phospholipid Monolayers on Protein Binding, Langmuir : the ACS journal of surfaces and colloids, 28 (2012) 9680-9688.

[48] D. Vollhardt, Morphology and phase behavior of monolayers, Advances in Colloid and Interface Science, 64 (1996) 143-171.
[49] J.M. Rodríguez Patino, C.C. Sánchez, M.R. Rodríguez Niño, Morphological and Structural Characteristics of Monoglyceride Monolayers at the Air−Water Interface Observed by Brewster Angle Microscopy, Langmuir : the ACS journal of surfaces and colloids, 15 (1999) 2484-2492.
[50] O. Maniti, M.F. Lecompte, O. Marcillat, B. Desbat, R. Buchet, C. Vial, T. Granjon, Mitochondrial creatine kinase binding to phospholipid monolayers induces cardiolipin segregation, Biophys J, 96 (2009) 2428-2438.
[51] Y. Guillemin, J. Lopez, D. Gimenez, G. Fuertes, J.G. Valero, L. Blum, P. Gonzalo, J. Salgado, A. Girard-Egrot, A. Aouacheria, Active Fragments from Pro- and Antiapoptotic BCL-2 Proteins Have Distinct Membrane Behavior Reflecting Their Functional Divergence, PloS one, 5 (2010) e9066.
[52] A.l.A.M. Santafé, L.c.J. Blum, C.A. Marquette, A.s.P. Girard-Egrot, Chelating Langmuir−Blodgett Film: A New Versatile Chemiluminescent Sensing Layer for Biosensor Applications, Langmuir : the ACS journal of surfaces and colloids, 26 (2009) 2160-2166.
[53] H.P. Ta, K. Berthelot, B. Coulary-Salin, B. Desbat, J. Gean, L. Servant, C. Cullin, S. Lecomte, Comparative studies of nontoxic and toxic amyloids interacting with membrane models at the air-water interface, Langmuir : the ACS journal of surfaces and colloids, 27 (2011) 4797-4807.
[54] M.N.G. de Mul, J.A. Mann, Determination of the Thickness and Optical Properties of a Langmuir Film from the Domain Morphology by Brewster Angle Microscopy, Langmuir : the ACS journal of surfaces and colloids, 14 (1998) 2455-2466.
[55] J. Saccani, S. Castano, F. Beaurain, M. Laguerre, B. Desbat, Stabilization of Phospholipid Multilayers at the Air−Water Interface by Compression beyond the Collapse: A BAM, PM-IRRAS, and Molecular Dynamics Study, Langmuir : the ACS journal of surfaces and colloids, 20 (2004) 9190-9197.
[56] C. Larios, J. Miñones, I. Haro, M.A. Alsina, M.A. Busquets, J. Miñones Trillo, Study of Adsorption and Penetration of E2(279−298) Peptide into Langmuir Phospholipid Monolayers, The Journal of Physical Chemistry B, 110 (2006) 23292-23299.
[57] J. Sarkis, J.F. Hubert, B. Legrand, E. Robert, A. Cheron, J. Jardin, E. Hitti, E. Le Rumeur, V. Vie, Spectrin-like Repeats 11-15 of Human Dystrophin Show Adaptations to a Lipidic Environment, Journal of Biological Chemistry, 286 (2011) 30481-30491.
[58] A. Girard-Egrot, J.-P. Chauvet, G. Gillet, M. Moradi-Améli, Specific Interaction of the Antiapoptotic Protein Nr-13 with Phospholipid Monolayers is Prevented by the BH3 Domain of Bax, Journal of Molecular Biology, 335 (2004) 321-331.
[59] L. Francois-Moutal, O. Maniti, O. Marcillat, T. Granjon, New insights into lipid-Nucleoside Diphosphate Kinase-D interaction mechanism: Protein structural changes and membrane reorganisation, Biochimica et Biophysica Acta (BBA) - Biomembranes, 1828 (2013) 906-915.
[60] J. Sarkis, J. Rocha, O. Maniti, J. Jouhet, V. Vié, M.A. Block, C. Breton, E. Maréchal, A. Girard-Egrot, The influence of lipids on MGD1 membrane binding highlights novel mechanisms for galactolipid biosynthesis regulation in chloroplasts, The FASEB Journal, (2014).
[61] S. Brot, C. Auger, R. Bentata, V. Rogemond, S. Ménigoz, N. Chounlamountri, A. Girard-Egrot, J. Honnorat, M. Moradi-Améli, Collapsin Response Mediator Protein 5 (CRMP5) Induces Mitophagy, Thereby Regulating Mitochondrion Numbers in Dendrites, Journal of Biological Chemistry, 289 (2014) 2261-2276.
[62] S. Redon, J. Massin, S. Pouvreau, E. De Meulenaere, K. Clays, Y. Queneau, C. Andraud, A. Girard-Egrot, Y. Bretonnière, S. Chambert, Red Emitting Neutral Fluorescent Glycoconjugates for Membrane Optical Imaging, Bioconjugate Chemistry, (2014).
[63] S. McLaughlin, D. Murray, Plasma membrane phosphoinositide organization by protein electrostatics, Nature, 438 (2005) 605-611.
[64] P. Strittmatter, J.M. Kittler, J.E. Coghill, J. Ozols, Interaction of non-myristoylated NADH-cytochrome b5 reductase with cytochrome b5-dimyristoylphosphatidylcholine vesicles, Journal of Biological Chemistry, 268 (1993) 23168-23171.